CHEMICAL ENGINEERING TRANSACTIONS
VOL. 70, 2018

A publication of
AIDIC
The Italian Association
of Chemical Engineering
Online at www.aidic.it/cet

Guest Editors: Timothy G. Walmsley, Petar S. Varbanov, Rongxin Su, Jiří J. Klemeš

ISBN 978-88-95608-67-9; **ISSN** 2283-9216

DOI: 10.3303/CET1870218

Mathematical Simulation of PEMFC Platinum Cathode Degradation Accounting Catalyst's Nanoparticles Growth

Eleonora M. Koltsiva[a,*], Violetta A. Vasilenko[a], Andrei I. Shcherbakov[a], Evgenia A. Fokina[a], Vera A. Bogdanovskaya[b]

[a]D.Mendeleev University of Chemical Technology of Russia, Miusskaya sq., 9, Moscow, 125047, Russia
[b]A.N. Frumkin Institute of Physical chemistry and Electrochemistry Russian Academy of Sciences, Leninsky prospect, 31, Moscow, 199071 Russia
kolts@muctr.ru

This paper presents a mathematical model of platinum catalyst degradation. Equation describing the degradation of electrochemical surface area on the base of mechanisms: platinum nanoparticles electrochemical dissolution, particle growth due to Ostwald ripening, migration of nanoparticles along the carbon support, coalescence of fine particles, diffusion of platinum ions in the ionomer and their escape into the membrane has been obtained for the first time. Calculations has been carried out for platinum catalysts of two types: commercial and synthesized over carbon nanotubes. As a result of this simulation the evolutions of the platinum particle size distribution vs time have been obtained, values of electrochemical surface area vs time have been calculated and compared to available experimental data. The model allows to predict the operating life of a fuel cell.

1. Introduction

The development of the catalysts for the fuel cells (FC) is a priority trend for the development of these current sources. Particular attention of researchers is aimed at increasing the activity and stability of the catalysts.

Up to date, the carbon support (carbon black)-based platinum catalysts is the only commercially available catalytic system that provides for successful functioning of the hydrogen-air fuel cells with proton-exchange polymer electrolyte (PEMFC). The disadvantage of this catalytic system is platinum catalyst degradation (dissolution and growth of platinum particles), corrosion of carbon support in polymer electrolyte in the result of the carbon material oxidation. Shao-Horn et al. (2007) mentions four mechanisms of electrochemical surface area (ECSA) of the FC platinum electrodes:

1) The platinum particles growth due to Ostwald ripening, based on the enlargement of individual platinum nanoparticles on the surface of the support (carbon), it may include electrochemical dissolution of small platinum particles, diffusion of dissolved small particles to large particles in the ionomer phase and the redeposition of dissolved platinum on large particles;
2) Coalescence of particles due to platinum crystals migration;
3) Detachment of platinum nanoparticles from the surface of the carbon support due to its corrosion and further agglomeration of particles;
4) Dissolution and redeposition of platinum monocrystals in the ionomer and the membrane as a result of chemical reduction of platinum ions with hydrogen molecules penetrating through the membrane, what leads to loss of platinum available for electrochemical reaction on the cathode.

At modelling degradation of polymer electrolyte fuel cells (PEMFC) Darling and Meyers (2003) suggest that the main mass losses of platinum occur due to its electrochemical dissolution. Their model describes Pt electrochemical dissolution, PtO formation and PtO chemical dissolution. Bi and Fuller (2008) proposed the model accounting Pt electrochemical dissolution and re-deposition in the cathode, Pt ion transport by diffusion and Pt ion chemical reduction in membrane by hydrogen that permeates from the anode. Ahluwalia et al. (2014) proposed a model combing non-ideal solid solution theory for Pt dissolution with the dynamics of particle size

Please cite this article as: Koltsova E.M., Vasilenko V.A., Shcherbakov A.I., Fokina E.A., Bogdanovskaya V.A., 2018, Mathematical simulation of pemfc platinum cathode degradation accounting catalyst's nanoparticles growth , Chemical Engineering Transactions, 70, 1303-1308 DOI:10.3303/CET1870218

evolution considering particle growth by Ostwald ripening and coalescence. Toyota Motor Corporation and the Japan Fine Ceramics Centre (JFCC) (2015) have developed a new observation technique that allows researchers to monitor the behaviour of nanometre-sized particles of platinum during chemical reactions in PEM fuel cells, so that the processes leading to reduced catalytic reactivity can be observed. This new approach allows the coarsening process to be observed in real time at all stages as electricity is generated. In presented video one can observe the growth of the platinum particles primarily due to their coalescence. Moein-Jahromi et al. (2017) presented an empirical based model for prediction the ECSA decline and the Pt particles radius growth under different cyclic load protocols. The outputs of this modeling were used in an agglomerate model of catalyst layer to forecast the catalyst loss after some cycles.

In our previous experimental study (Bogdanovskaya et al., 2016) higher corrosion resistance of catalysts synthesized on carbon nanotubes was confirmed. It was shown that platinum ECSA reduction was not exceed 15 % of its initial value. If in our previous work (Mitrichev et al., 2016) the forecast of the platinum catalyst ECSA fall was described by the regression equation, in this paper a mathematical model base on the equation describing the degradation of electrochemical surface area due to the mechanisms: platinum nanoparticles electrochemical dissolution, particle growth due to Ostwald ripening, migration of nanoparticles along the carbon support, coalescence of fine particles, diffusion of platinum ions in the ionomer and their escape into the membrane. It should be mentioned that such equation has been developed for the first time.

2. Experimental studies

Experimental researches on studying the platinum catalysts degradation mechanisms are carried out by Prof. Bogdanovskaya and others. Bogdanovskaya et al. (2016) have developed an effective liquid phase polyol synthesis method of monoplatinum catalyst on CNT, with platinum content of 20 wt %, which enables, in the model conditions, to obtain the platinum surface of 45 - 50 m^2/g and the activity in electroreduction oxygen reaction of ~ 50 A/g at the potential of 0.9 V, while maintaining high selectivity with regard to recovering oxygen to the water and higher stability. The study confirmed the higher corrosion stability of catalysts supported by carbon nanotubes. By means of a complex of electrochemical and structural techniques, it is shown that as regards their activity under model conditions and within membrane-electrode assembles, the catalysts synthesized by the polyol method 20Pt/CNT are close to commercial monoplatinum systems 20Pt/C(E-TEK) with the same mass content of platinum (20 wt %) and their corrosion stability is double that of commercial catalysts. The higher stability of catalysts supported by CNT as compared with 20Pt/C(E-TEK) was confirmed in their tests within the composition of membrane-electrode assembly (MEA).

To elucidate the mechanism of degradation of the platinum catalyst the effect of potential cycling on the platinum electrochemically active surface area was studied by the accelerated testing method (Bogdanovskaya et al., 2016).

3. Mathematical simulation of the catalyst ECSA degradation

At developing a mathematical model, it was assumed that the catalyst ECSA degradation on the cathode occurs only due to the reaction of platinum electrochemical dissolution/deposition:

$$\mathrm{Pt} \leftrightarrow \mathrm{Pt}^{2+} + 2e^- \tag{1}$$

The diffusion of platinum ions into the membrane and their interaction with hydrogen molecules coming from the anode are taken into account also:

$$\mathrm{H_2} + \mathrm{Pt}^{2+} \rightarrow \mathrm{Pt} + 2\mathrm{H}^+ \tag{2}$$

The rate of the direct reaction (W_1, mol/(m^2s)) and reverse reaction (W_{-1}, mol/(m^2s)) are determined by Eq(3-4):

$$W_1 = i_1/(nF) = k_1 a_{Pt}\, exp\left[(\alpha_a nF)(E_m - E_s - U_1)/(RT)\right] \tag{3}$$

$$W_{-1} = i_{-1}/(nF) = k_{-1}\left(C_{Pt^{2+}} / C^{ref}_{Pt^{2+}}\right) exp\left[-(\alpha_c nF)(E_m - E_s - U_1)/(RT)\right] \tag{4}$$

where i_1 – current density of the direct reaction (1), A/m^2; i_{-1} – current density of the reverse reaction (1), A/m^2; n – number of electrons in the reaction (1); F – Faradey constant, C/mol; k_1 –the direct reaction rate constant (1), mol/(m^2s); k_{-1} – the reverse reaction rate constant, mol/(m^2s); α_a – anode change transfer coefficient; α_c – cathode change transfer coefficient; R – universal gas constant J/(mol·K); E_m – metal phase potential, V; E_s – dissolved phase potential, V; U_1 – thermodynamically reversible electrode potential for reaction (1), V; $C_{Pt^{2+}}$ – concentration of platinum ions, mol/m^3; $C^{ref}_{Pt^{2+}}$ – equilibrium concentration of platinum ions, mol/m^3.

The expression for determining the electrode potential (Darling and Meyers, 2003):

$$U_1 = U_1^{eq} - \Delta\mu_{Pt}/(2F) \tag{5}$$

where U_1^{eq} – the standard electrode potential of the reaction (1), V; μ_{Pt} – Pt electrochemical potential, J/mol. The Kelvin equation proposed by Darling and Meyers (2003) is used to determine the electrochemical potential:

$$\Delta\mu_{Pt} = (\sigma_{Pt} M_{Pt})/(l\rho_{Pt}) \tag{6}$$

where σ_{Pt} – surface tension, J/m^2; M_{Pt} – molecular weight of platinum, kg/mol; l – platinum particle diameter, m; ρ_{Pt} – platinum density, kg/m^3.

Eq(6) takes into account the influence of the surface tension of the platinum crystal on the equilibrium potential. As platinum particles become larger, the shift in the chemical potential of platinum decreases.

In the result of simulation in an equation characterizing the change of platinum crystals number from time was obtained. At derivation of the equations it was considered that platinum particles can detach from carbon support, aggregate, dissolve as a result of an electrochemical reaction and re-precipitate (crystallize) by Ostwald mechanism.

If N is the number of platinum crystals with sizes from l to $l+dl$, then $\varphi(t, x, l)$ – is the density function of the platinum particles size distribution:

$$\varphi(t, x, l)\, dl = N\,[l, l + dl] \tag{7}$$

The correlation describing the platinum crystals reduction rate due to the electrochemical dissolution η_1 [m/s]:

$$\eta_1 = \frac{dl}{dt} = -\frac{M_{Pt}}{\rho_{Pt}} W_1 \tag{8}$$

The correlation describing the platinum crystals growth rate due to the electrochemical deposition by Ostwald mechanism η_2 [m/s]:

$$\eta_2 = \frac{dl}{dt} = \frac{M_{Pt}}{\rho_{Pt}} W_{-1} \tag{9}$$

The equation of the cluster population balance for the function of clusters size distribution, taking into account the mechanisms of cluster dissolution and crystallization, the diffusion and migration of clusters over the surface, the mechanism of coalescence of clusters there was developed for the first time in the form of:

$$\frac{\partial\varphi}{\partial t} - \frac{\partial\varphi\eta_1}{\partial l} + \frac{\partial\varphi\eta_1}{\partial l} = D_{Pt}\frac{\partial^2\varphi}{\partial x^2} + \int_0^{\frac{l}{2^{1/3}}} K\left(\mu, \sqrt[3]{l^3-\mu^3}\right)\varphi(\mu)\varphi\left(\sqrt[3]{l^3-\mu^3}\right)d\mu - \varphi(l)\int_0^L K(\mu, l)\varphi(\mu)d\mu \tag{10}$$

where D_{Pt} – the diffusion coefficient of platinum particles, m^2/s; μ (μ-phase) – a set of particles whose sizes belong to a segment $[\mu, \mu + d\mu]$; $K(\mu, l)$ – the aggregation (coalescence) constant, characterizing the probability of aggregation (coalescence) of particles with sizes equal to μ and l.

In Eq(10), the second and third terms on the left side characterize the change in the number of platinum nanoparticles due to electrochemical dissolution (the second term) and re-deposition (third term). On the right-hand side, the first term characterizes the migration of platinum nanoparticles along the surface of the carbon support, the second and third terms characterize the change in the number of particles due to coalescence. The second term on the right-hand side characterizes the coalescence of particles with sizes $\sqrt[3]{l^3-\mu^3}$ and μ, the third term characterizes the decrease in the number of particles of size l due to their aggregation (coalescence) with all other particles.

The equation of change of platinum ions concentration in the ionomer is described by Fick's second law:

$$\frac{\partial C_{Pt^{2+}}}{\partial t} = D_{Pt^{2+}}\nabla^2 C_{Pt^{2+}} + \frac{2D_{Pt^{2+}}F}{RT} div\left(C_{Pt^{2+}} grad E_s\right) - 4\pi\frac{\rho_{Pt}}{M_{Pt}}\int_0^L \varphi(\eta_1+\eta_2) l^2 dl \tag{11}$$

where $D_{Pt^{2+}}$ – platinum ions diffusion coefficient, m^2/s.

The Eq(11) accounts platinum ions Pt^{2+} diffusion into polymeric membrane from the catalytic layer (the first term on the right side), their migration under the influence of electric field (the second term) and formation/consumption for the platinum electrochemical dissolution.

For the integro-differential equation of the platinum nanoparticles clusters population balance a finite-difference splitting scheme based on the method of fractional steps has been developed. The time step Δt is divided into four parts. The difference scheme is divided into four sub-schemes. Each of the sub-schemes approximates a certain mechanism of ECSA degradation.

The program module is implemented by the authors in the programming language C ++.

To solve the equations initial and boundary conditions are given.

The initial condition for Eq(10):

$$\varphi(t=0, x, l) = \varphi^0(x, l) \tag{12}$$

The boundary conditions for Eq(10):

$$\varphi(t, x, l=L) = 0 \tag{13}$$

$$\varphi(t, x, l=l_n)\,\eta\,(t, x, l=l_n) = W_n \tag{14}$$

$$W_n = k_n\left(C_{Pt^{2+}} / C^{ref}_{Pt^{2+}}\right)^{m_1} \tag{15}$$

where l_n– nuclei-primary particle size, m; W_n – nucleation rate, m/s; k_n – nucleation rate constant, m/s.

To find the solution on the boundaries of the active layer, boundary conditions of the second type are given:

$$D_{Pt^{2+}}\left(\partial\varphi/\partial x\right)\Big|_{x=0} = 0 \tag{16}$$

$$D_{Pt^{2+}}\left(\partial\varphi/\partial x\right)\Big|_{x=X} = 0 \tag{17}$$

The initial condition for Eq(11):

$$C_{Pt^{2+}}(t=0, x) = C^0_{Pt^{2+}}(x) \tag{18}$$

The boundary conditions for Eq(11):

$$D_{Pt^{2+}}\left(\partial C_{Pt^{2+}}/\partial x\right)\Big|_{x=0} = 0 \tag{19}$$

$$D_{Pt^{2+}}\left(\partial C_{Pt^{2+}}/\partial x\right)\Big|_{x=X} = W_2 \tag{20}$$

where W_2 – the rate of platinum crystals formation reaction (2) in the membrane. As hydrogen is considered to be in the membrane in excess, so the speed W_2 can be written as follows:

$$W_2 = k_2\left(C_{Pt^{2+}}\right)^{m_2} \tag{21}$$

where k_2 – the rate constant of the platinum crystals formation reaction (2).

To write the difference scheme approximating Eq(10), a three-dimensional difference grid is introduced: time t, coordinate along the thickness of the active layer x, particle size l. Eq(10) is solved by the method of fractional steps.

The catalyst ECSA S_{act} [m^2_{Pt}/m^3] is calculated using the particle size distribution function:

$$S_{act}(t, x) = 4\pi\int_0^L \varphi(t, x, l)\, l^2 dl \tag{22}$$

The total number of particles is determined by the expression:

$$N(t) = \int_0^L \varphi(t, x, l)\, dl \tag{23}$$

The average particle size <l> is determined from expression:

$$\langle l\rangle = \left[N(t)\right]^{-1}\int_0^L \varphi(t, x, l)\, l\, dl \tag{24}$$

The initial particle size distribution is represented as a normal distribution.

4. Results of simulation

Simulation of the platinum cathode catalyst ECSA degradation was realized sequentially with the study of individual stages of the mechanisms.

During studying the only effect of the mechanism of platinum electrochemical dissolution it was found that at potential values below 1.2 V the influence of this mechanism is negligible. Its action begins to affect only for large values of the potential. Since the operating conditions of the cell are usually below the potential of 1.2 V, the contribution of this mechanism to the overall loss of the catalyst active surface will be negligible.

Table 1: List of the parameters used in the mathematical model

Parameter	Cathode catalyst	
	20PtE-TEK	20Pt (CNT+15 % XC72R)
The rate constants of the direct and reverse reaction of Pt dissolution, mol/(m^{2}s)	3.4e-12	3.4e-12
Nucleation constant	1e-35	1e-35
The reaction (2) rate constant, mol/(m^{2}s)	1e-10	1e-10
Coalescence constant, m^3/s	1e-17	5e-18
Platinum nanoparticles diffusion coefficient, m^2/s	1e-15	1e-15
Coefficient of platinum ions diffusion, m^2/s	1e-10	1e-10

It was found that under the operating conditions of the cell, the influence of only the platinum crystallization on degradation is generally negligible. At the same time, the change in the electrochemically active surface of the platinum catalyst due to the coalescence mechanism alone turned out to be significant.

The reaction's and coalescence constants were found by the scanning method. The values of the calculation parameters are shown in Table 1.

Figure 1 shows the effect of coalescence on the platinum nanoparticles size distribution after modeling of the different cycles number for two types of the catalysts.

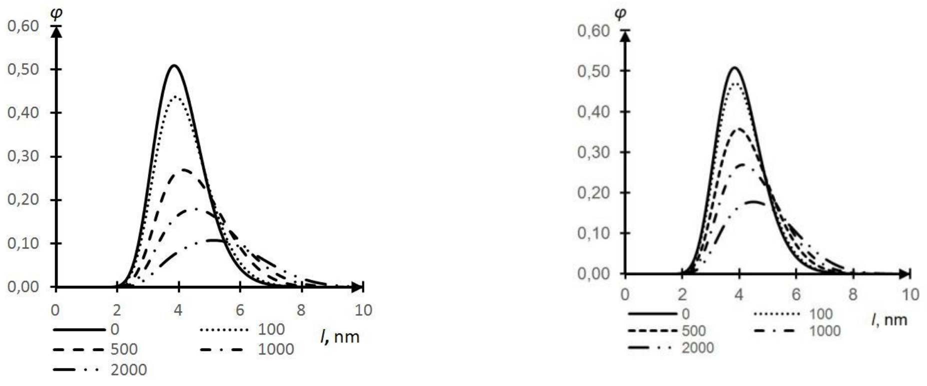

a

b

Figure 1: Particle size distribution at different number of cycles for the catalysts: a) 20PtE-TEK (0.42 mg$_{Pt}$/cm^2); b) 20Pt/CNT+15 % XC72 (0.50 mg$_{Pt}$/cm^2)

Table 2: The average particle size of platinum for various cathode catalysts

Parameter	20PtE-TEK		20Pt (CNT+15%XC72R)	
	0 cycles	2,000 cycles	0 cycles	2,000 cycles
Average particle size <*l*>, nm	4	5.4	4	4.5

Table 2 shows the calculated values of the average size of the platinum nanoparticles of cathode catalysts before potential cycling and after carrying out 2,000 cycles of accelerating tests. It can be seen from Figure 1 and Table 2 that with the potential cycles number increasing the most probable average sizes of the platinum nanoparticle size distribution function increase for commercial catalyst as well as for synthesized one, the average size of the platinum particle of the commercial catalyst is greater than of the CNT-based catalyst.

Figure 2 shows the experimental values of the catalysts active surface (dots), the values (curves 1, 2) calculated from the regression equation presented by Mitrichev et al. (2016) and the values (curves 1, 3) obtained from Eq.(22) as a function of cycles number, including at more cycles (5,000), at which tests were not conducted.

Curves1, 3 present calculated data for MEA with 20PtE-TEK cathode; 2, 4 – MEA with 20Pt/CNT+15 % XC72 cathode. From the Figure 2 one can see that at the potential cycling over 2,000 cycles the commercial catalyst ECSA is reduced by about 60 %, while for the CNT-based catalyst it is reduced by approximately 20 %. With the forecast for 5,000 cycles, the calculations showed that for long-term tests, catalytic systems made using nanotubes exhibit greater stability than commercial one. ECSA calculated by two methods are almost identical.

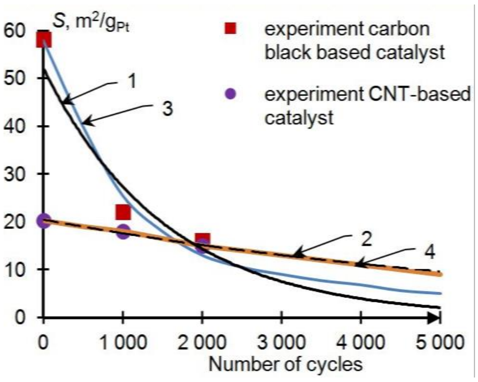

Figure 2: ECSA values at 5,000 cycles

5. Conclusions

The developed model includes the main mechanisms of degradation of the platinum catalyst: electrochemical dissolution of platinum nanoparticles, particle growth due to Ostwald ripening, migration of particles along the carbon support, coalescence of fine particles, diffusion of platinum ions in the ionomer and their transfer into the membrane. On the base of the mathematical model, it is possible to obtain the particle size distribution, the platinum ion concentration distribution vs time and thickness of the active layer. It is possible to predict the operating life of the fuel cell on the ECSA dependence on time. The simulation results show that the growth rate of platinum particles of the commercial catalyst is almost twice higher than for the catalyst synthesized on CNT. This again demonstrates the great stability of the catalytic systems manufactured using nanotubes in comparison with commercial ones synthesized on carbon black. It should be noted that the equation of the nanoclusters number population balance Eq(10), taking into account the growth, dissolution, diffusion and aggregation of clusters, was developed for the first time.

Acknowledgments

This study is partially supported by the state contract № 13.10932.2018/10.11.

References

Ahluwalia R.K., Arisetty S., Peng J.K., Subbaraman R., Wang X., Kariuki N., Myers D.J., Mukundan R., Borup R., Polevaya O., 2014, Dynamics of particle growth and electrochemical surface area loss due to platinum dissolution, Journal of The Electrochemical Society, 161, 291-304.

Bi W., Fuller T.F., 2008, Modeling of PEM fuel cell Pt/C catalyst degradation, Journal of Power Sources, 178(1), 188-196.

Bogdanovskaya V.A., Kol'tsova E.M., Tarasevich M.R., Radina M.V., Zhutaeva G.V., Kuzov A.V., Gavrilova N.N., 2016, Highly active and stable catalysts based on nanotubes and modified platinum for fuel cells, Russian Journal of Electrochemistry, 52(8), 723-734.

Darling R.M., Meyers J.P., 2003, Kinetic model of platinum dissolution in PEMFCs, Journal of the Electrochemical Society, 150(11), 1523-1527.

Mitrichev I., Vasilenko V., Scherbakov A., Koltsova E., 2016, Simulation of PEMFC with Pt/CNT nanostructured cathode catalyst, Chemical Engineering Transactions, 52, 1003-1008.

Moein-Jahromi M., Kermani M.J., Movahed S., 2017, Degradation forecast for PEMFC cathode-catalysts under cyclic loads, Journal of Power Sources, 359, 611-625.

Shao-Horn Y., Sheng W.C., Ferreira P.J., Holby E.F., Morgan D., 2007, Instability of supported platinum nanoparticles in low-temperature fuel cells, Top Catal, 46(3), 285-305.

Toyota, JFCC breakthrough in real-time observation of fuel cell catalyst degradation, 2015, Fuel Cells Bulletin, 6, 14-15.